MATERIALS

Organic Transistor (OFET) Materials

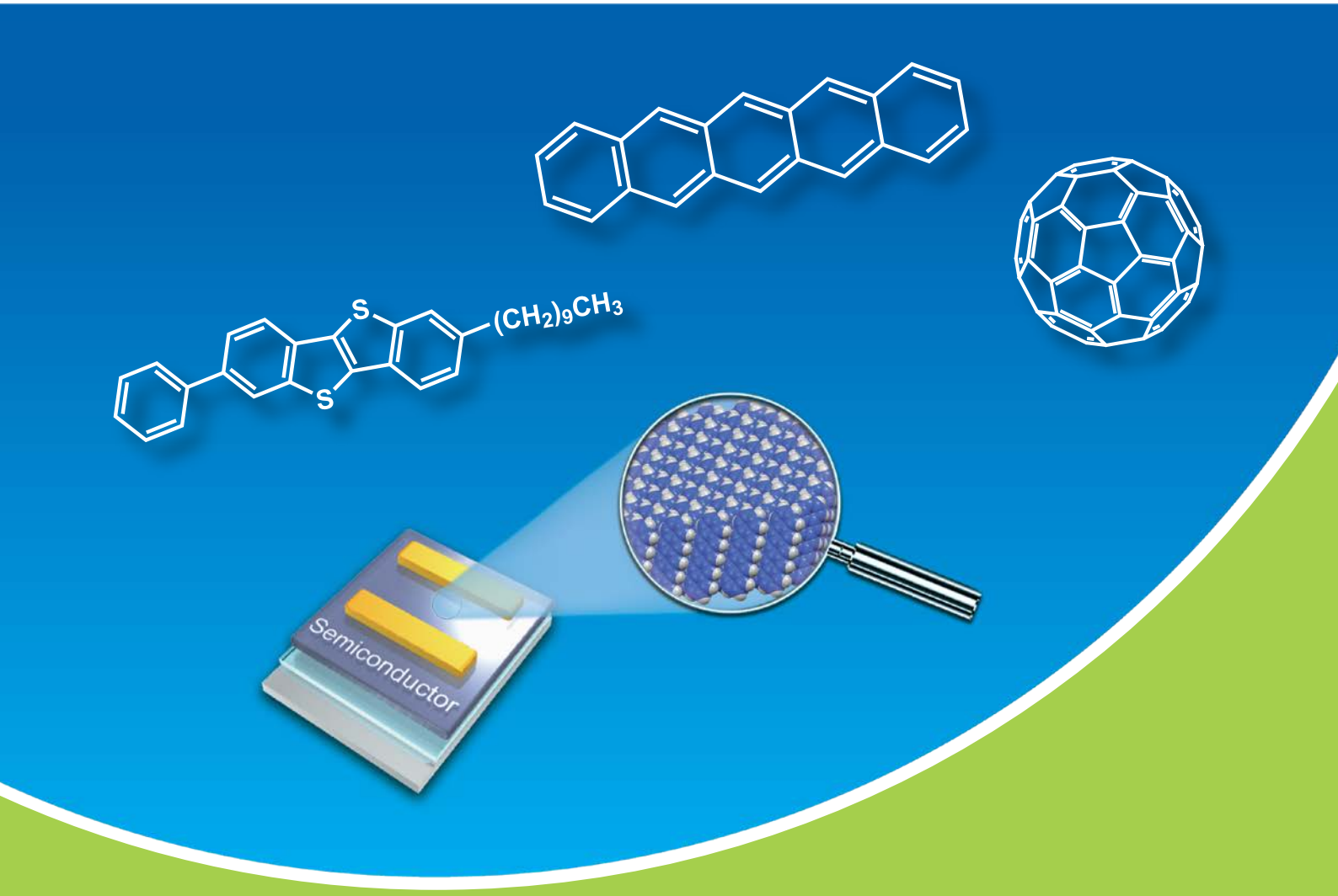

High Quality Organic Semiconductor Materials

p-Type Organic Semiconductors

n-Type Organic Semiconductors

Ambipolar Semiconductors

Liquid Crystalline Semiconductors

Organic Transistor (OFET) Materials

Organic field-effect transistors (OFETs) are promising components for the next-generation electronic devices. In 1984, OFET research began with the first report of mobility in a merocyanine dye-based field-effect device by Kudo *et al.*[1] Since high hole mobility (1.5 cm^2/Vs), which comparable to that of amorphous silicon, was achieved using a pentacene-based OFET device in 1997,[2] the possibility of a practical application of OFET's became realistic and the research field became quite popular worldwide. While silicon has performed well in devices, the inorganic nature of them prohibits flexible structures. As a result, OFETs have attracted much attention for their potential to be flexible, thin and light-weight, which could be applicable for foldable electronic circuits and implantable biometric sensors. [3, 4]

A noted potential application with OFET's involves their "printability". Printed electronics are an innovative technology for mass and low cost device productions, which could allow for the production of high density and large circuits on flexible substrates such as paper and plastic films. A fusion of "Printed electronics" and "Organic transistors" could offer especially promising technology by allowing for low cost and large scale manufacture of various functional devices. [5-7]

One of the functional parameters evaluated in organic semiconductor materials is mobility (μ), which indicates how fast the holes (p-type) or electrons (n-type) within the semiconducting layer move. A material that possesses high carrier mobility is required for producing high-speed circuits. OFET devices are a largely simple construction containing an organic semiconductor layer, an insulating layer, and source-drain-gate electrodes. These components allow for the evaluation of fundamental transistor parameters including mobility, operation voltage, and driving stability.

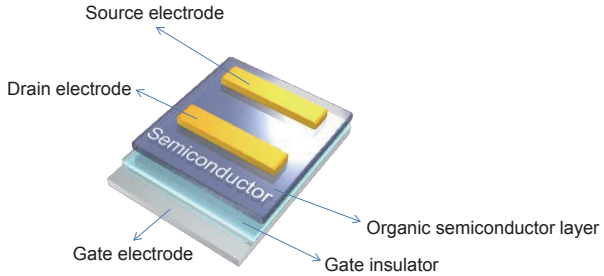

Top view

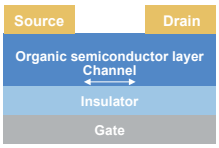

Side view

Due to the expanded π-conjugated system within organic semiconductor molecules, these often produce large intermolecular interactions inducing an improvement in the mobility within OFET devices. In general, the expansion and extension of π-conjugation is an effective strategy in the molecular design of OFET molecules and polymers. As an example, Pentacene, which consists of 5 fused benzene rings, possesses superior electrical properties compared to that of Tetracene, which consists of 4 fused benzene rings. [8] However, a linear increase in the number of fused aromatic rings in a simple hydrocarbon system raises the Highest Occupied Molecular Orbital (HOMO), resulting in a critical decrease in the air-stability of the molecule and semiconductor materials. [8] This trade-off issue between the mobility and the air-stability of the materials has been a key problem to overcome. Given this context, in 2006 DPh-BTBT **[D3526]**, a thienothiophene-fused organic compound, had been reported by Takimiya *et al.,* as an innovative OFET material.[9] DPh-BTBT features a deep HOMO level (-5.6 eV), which leads to remarkable air-stability during OFET device performance, and the HOMOs are well-distributed over the sulfur atoms of the thienothiophene moieties inducing good hole carrier transport. DPh-BTBT-based FET devise further achieved excellent electrical properties with a high hole mobility of 2.0 cm^2/Vs. Followed by the innovation and molecular design of DPh-BTBT, Ph-BTBT-10, an smectic E (SmE) liquid crystalline material, was recently reported by Hanna *et al.,* as a p-type material that bears an asymmetric structure in which the alkyl and the phenyl group are substituted on one side of the benzothienobenzothiophene (BTBT) moiety.[10] Additionally, Ph-BTBT-10 can be handled in solution processing such the spin-coting method, and possesses both good heat-resistance and film-forming properties. The Ph-BTBT-10 spin-coated devise exhibited not only outstanding OFET performance with ultra-high mobility (μ_{max} = 14.7 cm^2/Vs), but also comparable to oxide semiconductors (IGZO) with remarkable air-stability.

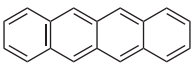

Tetracene
[N0951]

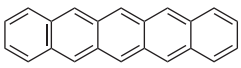

Pentacene
[P2524]

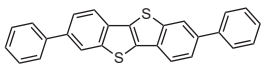

DPh-BTBT
[D3526]

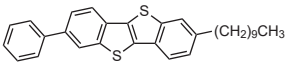

DPh-BTBT-10
[D5491]

One of the largest benefits of organic compounds for OFET's is their immense structural variety. This variety can be used to control the various properties they possess such as the electrical performance, stability, and processing characteristics through the chemical modification of the molecular units. Within the organic transistor research field, the possibilities for practical application has dramatically improved by introducing new concepts and various materials proposals, including the unique OFET materials and the parent molecules used to create them.

● High Quality Organic Semiconductor Materials (For Organic Electronics)

TCI offers “High Quality Organic Semiconductor Materials (For Organic Electronics)” specialized for electrical performance such as OFET mobility*. A material used in the active layer of an OFET device requires exceptionally high-purity to produce good OFET function. However, it is difficult to analytically (HPLC, GC, etc.) determine the purity at the ultra-high levels required for OFET function. To surmount this quality assurance challenge, we have begun in-house fabrication of OFET devices using our OFET materials. Once fabricated, we assess the functionality of the OFET as a quality assurance measure to confirm the electronic properties and device performance of the “High Quality Organic Semiconductor Materials (For Organic Electronics)”. We constantly seek to improve our technology and skill in order to provide high-purity and quality materials our customers.

(*The mobility refers to device evaluation measurements obtained within our facility under environment condition.)

Results of the device test are fed buck to the synthesis and purification process

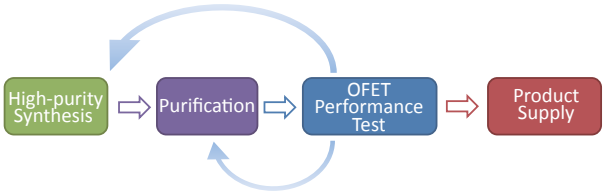

List of High Quality Organic Semiconductor Materials (For Organic Electronics)

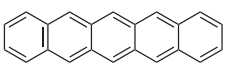

Pentacene
[P2524]

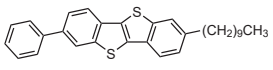

Ph-BTBT-10
[D5491]

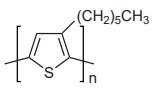

P3HT
[P2513]
M_n: 36,000 ~ 45,000
RR: > 99.0%

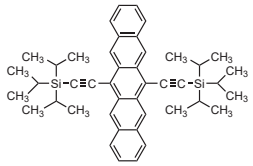

TIPS Pentacene
[B5942]

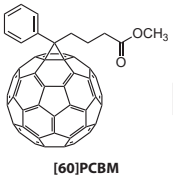

[60]PCBM
[P2682]

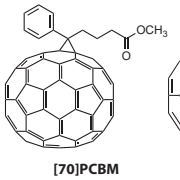

[70]PCBM
[P2683]

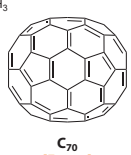

C_{70}
[F1233]

Compound	Product No.	Specification		
		Purity (%)	Mobility (cm^2/Vs)	Si/SiO_2 Substrate Surface Condition
Pentacene	P2524	> 99.999	> 0.35	Bare
Ph-BTBT-10	D5491	> 99.5	> 10.0	ODTS
P3HT	P2513	Pd: < 100ppm	> 0.10	OTS
TIPS Pentacene	B5942	> 99.0	> 0.10	HMDS
C_{70}	F1233	> 99.0	> 0.30	HMDS
[60]PCBM	P2682	> 99.5	> 0.020	HMDS
[70]PCBM	P2683	> 99.0	> 0.015	HMDS

1. An Example of OFET Evaluation 1: Typical p-type Material "Pentacene"

Pentacene [P2524]

(99.999%, trace metals basis) (purified by sublimation)

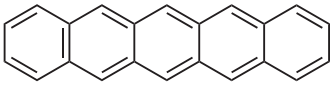

Pentacene
[P2524]

Pentacene, a simple polyaromatichydrocarbon, has been studied for its fundamental properties and applications in organic electronic research.[11, 12] In particular, many research studies have been conducted to evaluate its potential as a carrier transporter within OFET devices.[2,13] TCI provides two subliminally purified pentacene reagents: P2524 and P0030. P2524 (99.999% trace metal basis) is our high-quality grade reagent, which has additional specifications for its OFET mobility: [> 0.35 cm^2/Vs (bare Si/SiO_2)]. We inspect P2524 through the OFET evaluation process in every product lot. Only lots that pass this functional test are packed and shipped as “High Quality Organic Semiconductor Materials (For Organic Electronics)”.

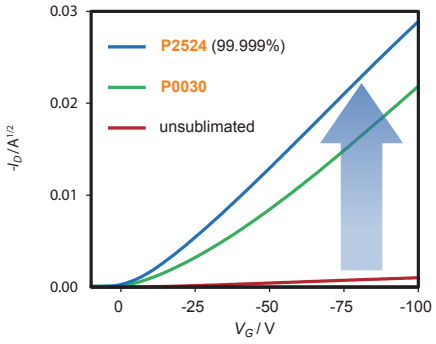

Figure 1. Transfer curves of various grades of pentacene.

Table 1. OFET characteristics of the pentacenes.

Product No.	Sample grade	Substrate	Mobility (cm^2/Vs)	V_{th} (V)
-	Pentacene (non-sublimation)	Si/SiO_2 (bare)	5.3×10^{-4}	-13
P0030	Pentacene (purified by sublimation)	Si/SiO_2 (bare)	0.29	-22
P2524	Pentacene (99.999%, trace metals basis) (purified by sublimation)	Si/SiO_2 (bare)	0.39	-10

The performances of the pentacene-based OFET devices are summarized in Table 1 and Figure 1. These devices were fabricated via vacuum deposition method on bare Si/SiO_2 substrate without Self-Assembled Monolayer (SAM) treatment, the characteristics of which were measured under nitrogen conditions. Our sublimed pentacene **[P2524]** showed a large increase OFET performance compared to that of the non-sublimed pentacene. As a result, **P2524** (99.999% trace metal basis) showed an excellent OFET performance with the highest hole mobility of 0.39 cm^2/Vs. In comparison to other companies' sublimed pentacene samples, **P2524** (99.999% trace metal basis) possesses the highest drain current and the best OFET potential (Figure 2 and Table 2).

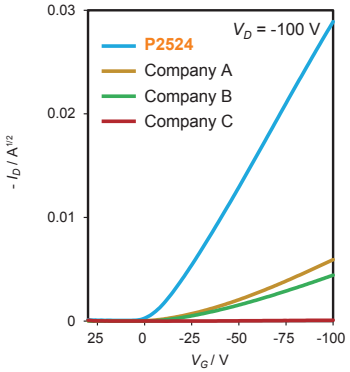

Figure 2. Transfer curves of OFET devices using several companies' pentacene.

Table 2. OFET characteristics of the pentacenes.

	Substrate	Mobility (cm^2/Vs)	V_{th} (V)
P2524	Si/SiO_2 (bare)	**0.39**	**-10**
Company A (sublimed)	Si/SiO_2 (bare)	0.002	-25
Company B (sublimed)	Si/SiO_2 (bare)	0.001	-25
Company C (sublimed)	Si/SiO_2 (bare)	5.0×10^{-6}	-23

1-a. Optimization of pentacene-based OFET devices

We have examined and optimized the functional preformance of pentacene-based OFET devices via substrate surface modification. The field-effect mobility of pentacene was measured using top-contact thin-film field-effect transistors geometry (Figure 3). The thin film of pentacene **[P2524]** as the active layer (60 nm) was vacuum-deposited onto Si/SiO_2 substrate (bare) or *n*-Octyltrichlorosilane (OTS) **[O0168]** -treated Si/SiO_2 substrate at room temperature (T_{sub} = RT). The drain and source electrodes (40 nm) were then prepared by gold evaporation through a shadow mask on top of the pentacene film; the drain-source channel length (L) and width (w) were 50 μm and 1.5 mm, respectively. The characteristics of the OFET devices were measured under nitrogen conditions.

The performances of the OFET devices are summarized in Table 3 and figure 4. All pentacene -based devices exhibited pure typical p-channel field-effect transistor (FET) characteristics. The FET performance were significantly improved by the SAM treatment; the OTS-treated device demonstrated the highest performance with a hole carrier mobility of 1.52 cm^2/Vs and an on/off ratio of 1.5×10^7 (Figure 4).

Figure 3. Illustration for the device structure of pentacene-based OFET device.

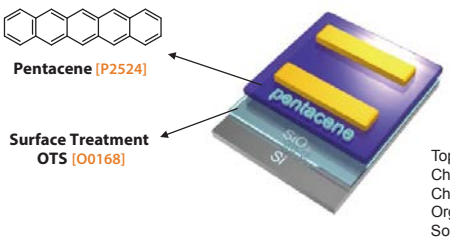

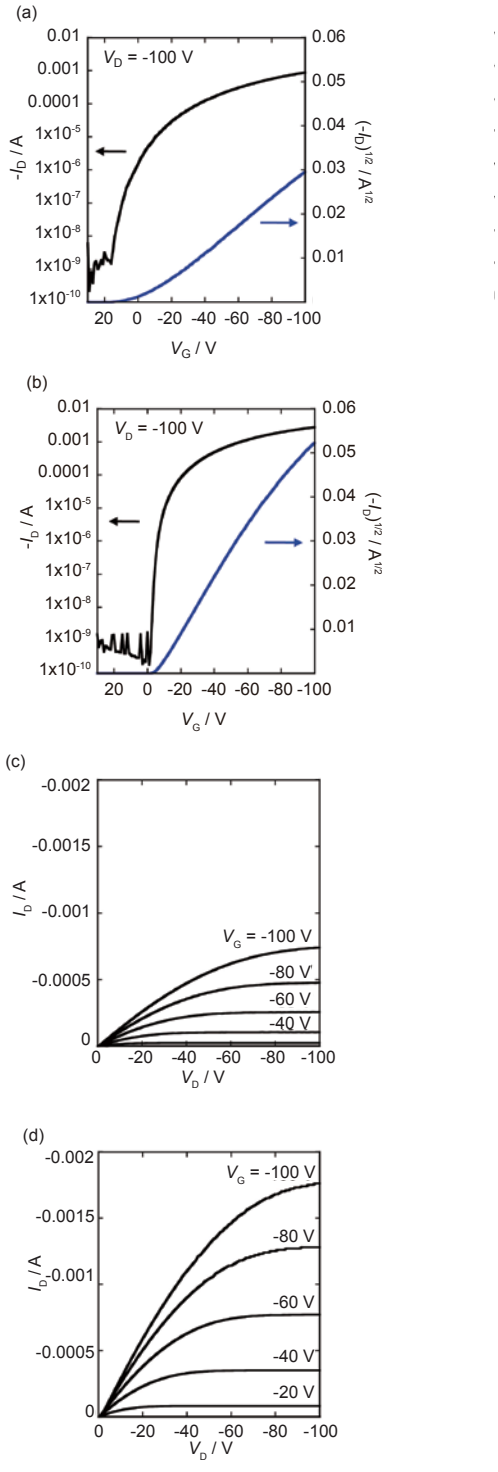

Figure 4. Typical OFET characteristics of top-contact devices fabricated using pentacene **[P2524]**.
(a, c) bare. (b, d) OTS-treated substrate.
(a, b) Transfer curves in the saturated region.
(c, d) Output curves at different gate voltages.

Table 3. OFET characteristics of P2524-based devices.

Compound	SAM	T_{sub} (°C)	Mobility (cm²/Vs)	V_{th} (V)	on/off
Pentacene [P2513]	bare	RT	0.35 ~ 0.37	-5.3	3.9 × 10^5
	OTS [O0168]	RT	1.50 ~ 1.52	-5.7	1.5 × 10^7

1-b. AFM images and XRD analysis

To clarify the pentacene thin film morphology and conformation, atomic force microscope (AFM) and X-ray diffraction (XRD) measurement were carried out (Figure 5). Regardless of either bare or OTS-treated substrate, highly regular terrace structures were observed (Figure 5a). In addition, XRD measurements of the pentacene films showed a series of peaks assignable to (00h) reflections; and the diffraction peak at $2\theta = 5.72°$ corresponds to a *d*-spacing of 15.5 Å (Figure 5b). These results demonstrated that the pentacene molecules stood nearly perpendicular to the substrate (thin-film-phase) in the film form. [12, 13]

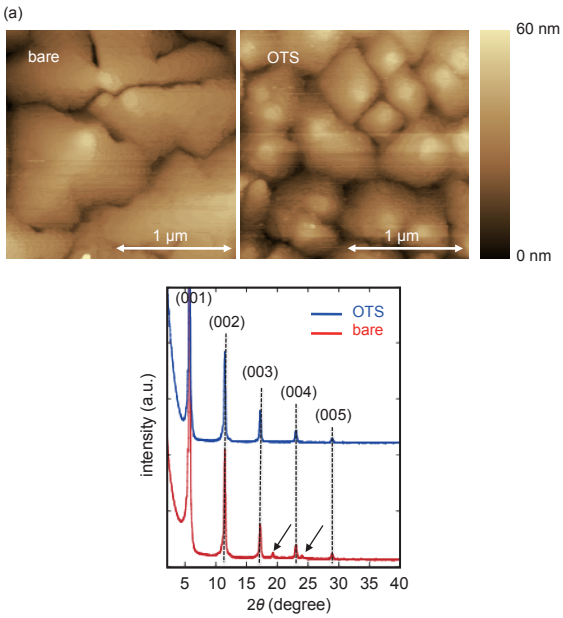

Figure 5. AFM images(a). and XRD analysis(b) of pentacene filims.

In the bare device (without SAM), two weak peaks assignable to face-on orientation were observed (Figure 5b, black arrow), which would create the disadvantage of carrier passes parallel to the substrate (Figure 6a). In contrast, such peaks were not observed in the pentacene film on the OTS-treated substrate (Figure 6b). It is one reason why the mobility was higher in the OTS-treated OFET device.

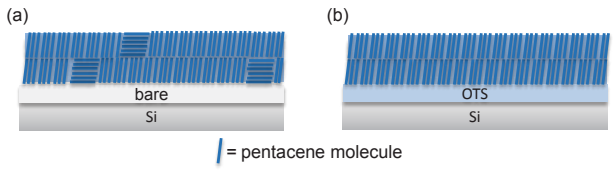

Figure 6. Orientation images of pentacene thin film form.

2. An Ultra-high Performance p-type Semiconductor Material "Ph-BTBT-10"

Ph-BTBT-10 (= 2-Decyl-7-phenyl[1]benzo-thieno[3,2-*b*][1]benzothiophene) [D5491]

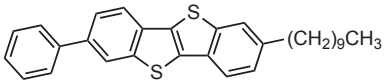

Ph-BTBT-10
[D5491]

Ph-BTBT-10, an SmE liquid crystalline material, has been recently reported by Hanna *et al.,* as a p-type material which possesses excellent transport properties.[10] Ph-BTBT-10 exhibits ultra-high mobility (μ_{max} = 14.7 cm²/Vs) comparable to oxide semiconductors (IGZO), and remarkable air stability. TCI has recently commercialized Ph-BTBT-10 as an ultra-high mobility and air stability p-type OFET material, and has begun evaluation via the fabrication and performance measurement of Ph-BTBT-10-based OFET devices using vacuum deposition methods in our laboratories. The devise showed a hole carrier mobility up to 14.0 cm²/Vs. Please see below for details.

2-a. Fabrication and evaluation of Ph-BTBT-10-based OFET device

The field-effect mobility of Ph-BTBT-10 was measured using top-contact thin-film field-effect transistors geometry (Figure 7). The thin film of Ph-BTBT-10 as the active layer (40 nm) was vacuum-deposited onto Si/SiO_2 substrate (bare) or Octadecyltrichlorosilane (ODTS) [O0079]-treated Si/SiO_2 substrate while heating the substrate. The drain and source electrodes (40 nm) were then prepared by gold evaporation through a shadow mask on top of the Ph-BTBT-10 film; the drain-source channel length (*L*) and width (*w*) are 50 μm and 1.5 mm, respectively. After deposition, these devices were thermal annealed at T_{sub} = 120 °C for 5 min under ambient conditions, and the characteristics of the OFET devices were measured.

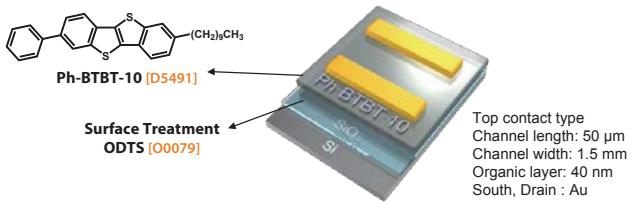

Figure 7. Illustration for the device structure of Ph-BTBT-10-based OFET.

The performances of the OFET devices are summarized in Table 4 and Figure 8. All Ph-BTBT-10-based devices exhibited pure typical p-channel field-effect transistor (FET) characteristics. The FET mobilities were quite dependent on the thermal annealing treatment regardless of the self-assemble-monolayer (SAM)

(Figure 8). This would be attributed to the phase transition from a monolayer to a bilayer crystal structure in the thin-film form. [10] The device fabricated on bare substrate demonstrated good performance with a hole carrier mobility of 4.86 cm^2/Vs and threshold voltage (V_{th}) of -8 V. Moreover, although V_{th} increased, the ODTS-treated devise showed the highest transport performance with a hole carrier mobility of 14.0 cm^2/Vs.

Table 4. OFET characteristics of the Ph-BTBT-10-based devices

Compound	SAM	Annealing Temp. (°C)	Mobility (cm^2/Vs)	V_{th} (V)
Ph-BTBT-10 [D5491]	bare	w/o	0.87 ~ 0.91	-24
		120	4.24 ~ 4.86	-8
	ODTS [O0079]	w/o	1.40 ~ 1.42	-23
		120	**10.3 ~ 14.0**	-22

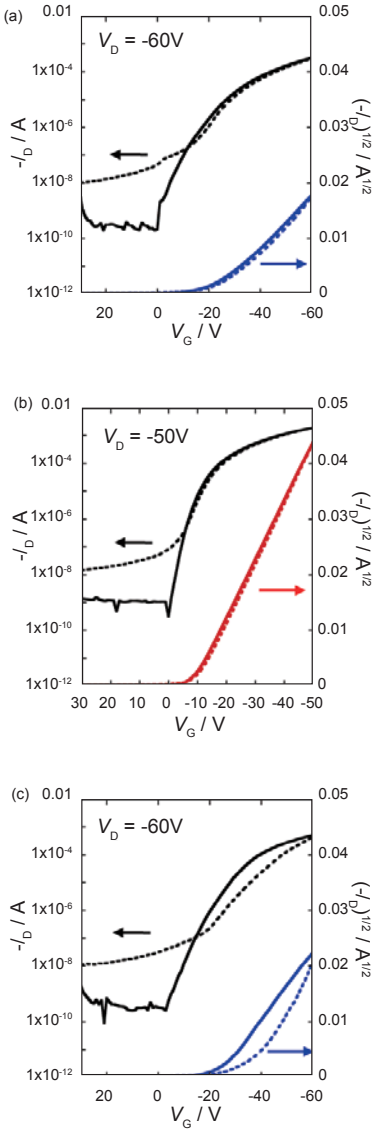

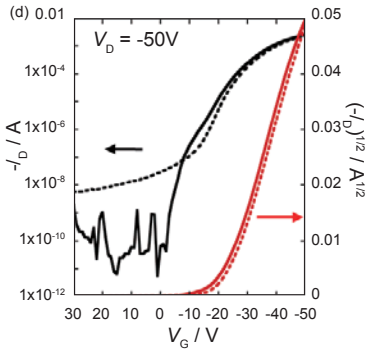

Figure 8. Transfer curves of the Ph-BTBT-10-based OFET devices.
(a) w/o annealing (bare) (b) annealing 120°C, 5min (bare)
(c) w/o annealing (ODTS) (d) annealing 120°C, 5min (ODTS)

2-b. 2D-GIXD Analysis

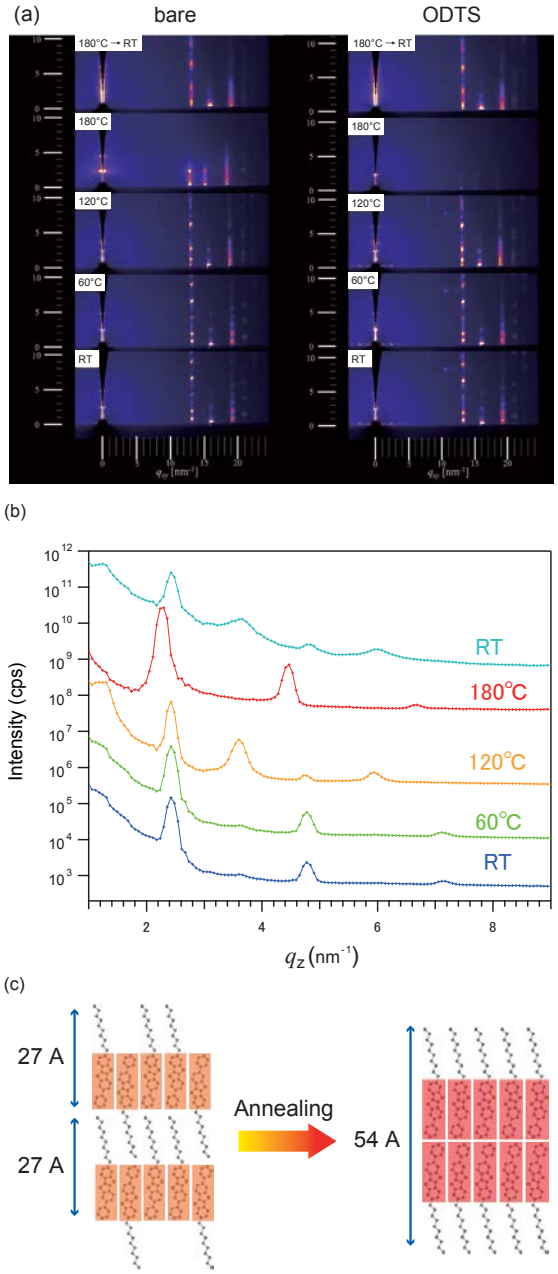

Figure 9. (a) 2D-GIXD analysis (Thermal in situ mesurement),
(b) 2D-GIXD analysis (Out-of-plane, bare substrate),
(c) Phase transition images of Ph-BTBT-10

The crystal structures of Ph-BTBT-10 thin films were analyzed by 2D-GIXD using synchrotron radiation. Figure 9 (a) and (b) display the thermal *in situ* 2D-GIXD data at different temperatures. The Ph-BTBT-10 films at RT and 60°C showed a similar series of peaks assignable to a monolayer structure with a *d*-spacing of 27 Å. When the substrate temperature was increased to 120°C, the diffraction peaks clearly changed, which suggested a transformation from a monolayer structure (d = 27 Å) into a bilayer structure with a *d*-spacing of 54 Å as shown in Figure 9 (c). Since the phase transition temperature to the SmE mesophase is 144°C, [10] a series of peaks assignable to SmE were observed when heated to 180°C. In addition, a mixed layer of monolayer and bilayer structures appeared when the Ph-BTBT-10 thin film was rapidly cooled from 180°C to RT. These results indicate that under these conditions the cooling speed might be a significant factor in forming a well-uniformed crystalline thin film structure. Based on these results, Ph-BTBT-10 can be handled through vacuum deposition method, and the phase transition from the monolayer to the bilayer structure can occur in the same way in which it occurs for solution processed Ph-BTBT-10 thin films. [10] Finally, we demonstrated top-ranked FET performances via vacuum deposition process using our in-house equipment.

3. Performance Evaluation of Highly Regioregular "P3HT"

P3HT
(= Poly(3-hexylthiophene-2,5-diyl))
(regioregular) **[P2513]**

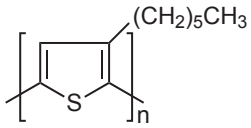

P3HT
[P2513]

TCI's P3HT (Poly(3-hexylthiophene-2,5-diyl)) **[P2513]** features a very high regioregularity (RR > 99%), a narrow molecular weight distribution (Mn = 36k ~ 45k), and a low metal content ratio (Pd < 100 ppm) in order to provide high quality solution-processed organic materials for organic electronics. The synthesis was conducted via the direct aryration polymerization (DArP) method in collaboration with Prof. Fumiyuki Ozawa at Institute for Chemical Research, Kyoto University.[14, 15]

We fabricated organic thin-film transistor (OFET) devices to validate and demonstrate hole transport properties of P3HTs. By comparing OFET characteristics of six P3HT samples including **P2513**, we revealed a correlation between OFET performances and (1) molecular weights and (2) regioregularities of P3HTs. As the result, the **P2513** devise showed the highest hole mobility, among the other P3HT devices. This suggested that the carrier transport property of P3HT was improved by both the regioregularity and the molecular weight of polymer parameters. In particular, the regioregularity could be considered the most significant factor for enhancing the electrical properties of P3HT in an OFET devise.

3-a. Fabrication and Evaluation of P3HT-based OFET devices

The hole mobility of **P2513** was measured using top-contact OFET geometry (Figure 10). The P3HT **[P2513]** was dissolved in chloroform:trichlorobenzene at a concentration of 10 mg/ml. The solution of **P2513** was spin-coated (1500 RPM) onto *n*-Octyltrichlorosilane (OTS) **[O0168]** -treated Si/SiO_2 substrate in a nitrogen glove box, then thermally annealed for 30 min. A gold layer with 40 nm thickness was deposited in vacuum chamber to serve as drain and source electrodes through a shadow mask on top of the **P2513** film; the drain-source channel length (L) and width (W) are 50 µm and 1.5 mm, respectively. The characteristics of the OFET devices were measured under nitrogen conditions. The other five P3HTs were also evaluated under the same protocol.

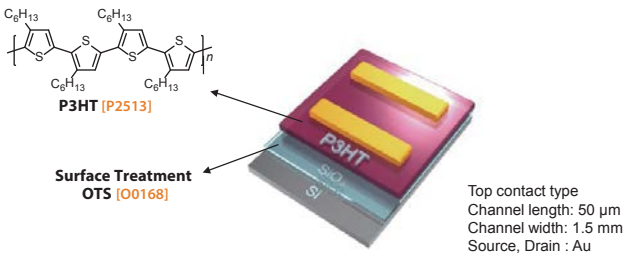

Figure 10. Illustration for the device structure of P3HT-based OFET.

3-b. A correlation between the hole transport mobility and the molecular weight18)

The device performances of **P2513** (high molecular weight Mn: 40K) and the other three P3HT samples having low molecular weights (Mn: 8K~28K), are summarized in Figure 11 and Table 5. Samples 1 and 2 were synthesized via the same DArP method same as with **P2513**.

The OFET performances of P3HT-based devices were improved by increasing the molecular weights of P3HT. In the case of **P2513**, the device achieved the highest transport performance with a hole mobility of 0.1 cm^2/Vs and an on/off ratio of 9×10^4. The high molecular weight could enhance a crystallinity of P3HT in the film form, that could be a reason why **P2513** possesses the excellent performances of OFET. The molecular weight of **P2513** was set 30K ~ 45K as a specification.

Table 5. Properties of P3HTs and mobility of OFET devices.

	RR (%)	M_n	Mobility ($\times 10^{-2}$ cm^2/Vs)
P2513	**99**	**40K**	**10.5±0.4**
Sample 1	99	18K	5.9±0.3
Sample 2	99	8K	3.0±0.4
Sample 3	98	28K	6.5±0.7
Sample 4	91	39K	1.2±0.1
Sample 5	93	-	1.7±0.3

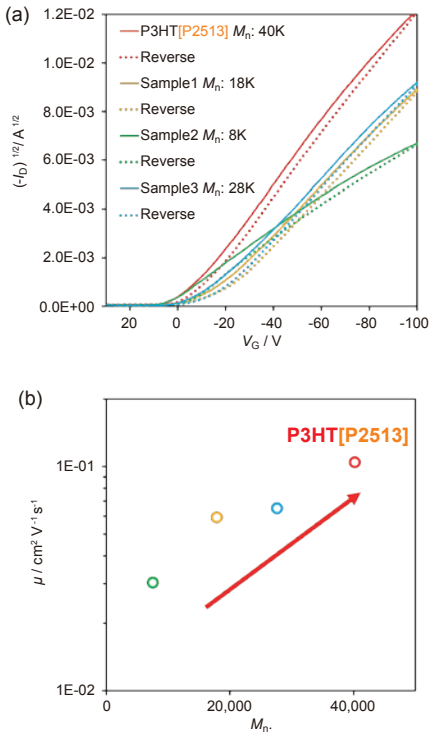

Figure 11. (a) Transfer curves of P3HT-based devices differ from molecular weight of P3HT, (b) A correlation between the hole transport mobility and the molecular weight.

3-c. A correlation between the hole transport mobility and the regioregularity[19)]

The device performances of **P2513** (the high regioregularity >99%) and the other two P3HT samples having low regioregularities (91, 93%) are summarized in Figure 12 and Table 5. Samples 4 and 5 indicate other companies' P3HT. The OFET performances of P3HT-based devices were drastically improved with increasing the regioregularities within P3HTs. While sample 4 (RR: 91%, Mn: 39K) displayed a high molecular weight as **P2513** (Mn: 40K), the hole transport mobility of the sample 4-based device was lower than that of the sample 2 (RR: 99%, Mn: 8K) -based device. From these results, the OFET performances of P3HT could be enhanced by the regioregularity rather than the molecular weight of P3HT.

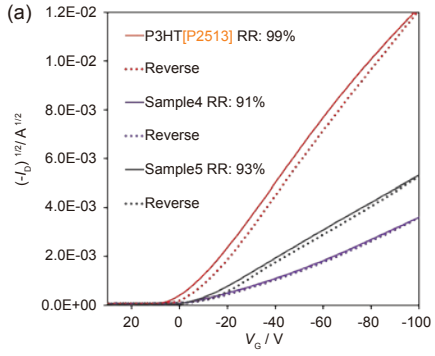

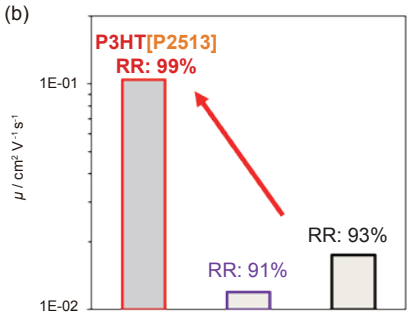

Figure 12. (A) Transfer curves of P3HT-based devices differ from regioregularity of P3HT, (b) A correlation between the hole transport mobility and the regioregularity.

Acknowledgments

A part of atomic force microscope (AFM: SPM-9700) was conducted at the AIST Nano-Processing Facility, supported by "Nanotechnology Platform Program" of the Ministry of Education, Culture, Sports, Science and Technology (MEXT), Japan. Portions of the X-ray diffraction (XRD: Smart Lab) was conducted at Advanced Characterization Nanotechnology Platform of the University of Tokyo, supported by "Nanotechnology Platform" of the Ministry of Education, Culture, Sports, Science and Technology (MEXT), Japan. 2D-GIXD experiments were performed at the BL46XU and BL19B2 of SPring-8 with the approval of the Japan Synchrotron Radiation Research Institute (JASRI) (Proposal No. 2017B1817 and 2017B1629). We acknowledge Prof. Noriyuki Yoshimoto, Assist. Prof. Daiki Kuzuhara and Mr. Shimpei Miura (Iwate Univ.), Assist. Prof. Mitsuharu Suzuki (NAIST) and Dr. Tomoyuki Koganezawa (JASRI) for technical support in GIXD.

Fundamental properties of Organic Transistor Materials

UV-vis absorption spectra (using in-house equipment)

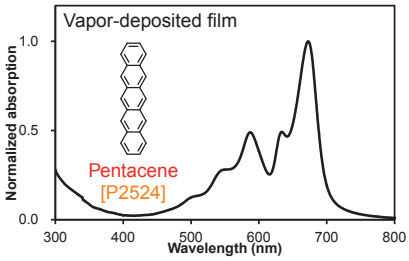

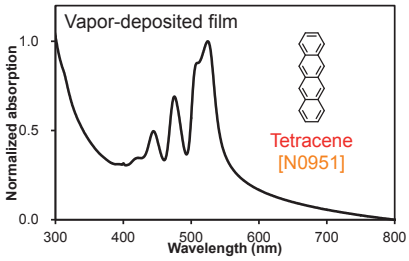

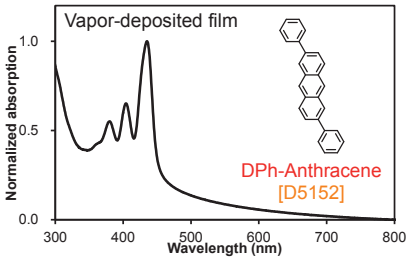

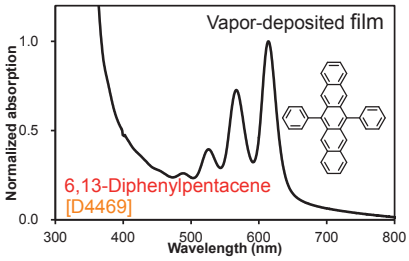

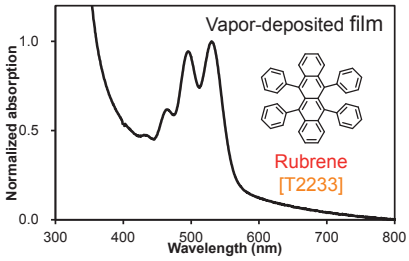

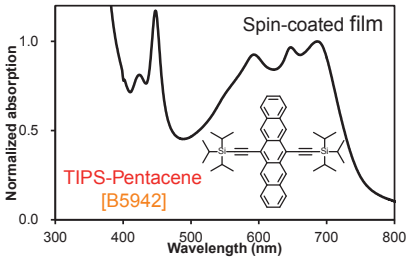

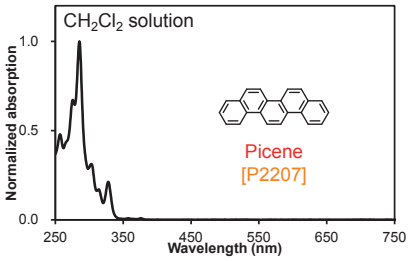

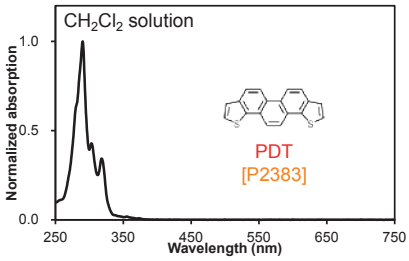

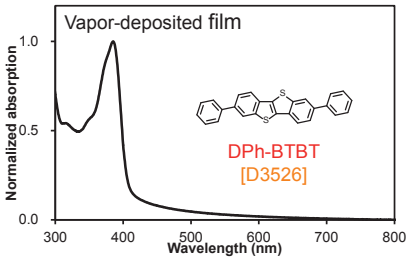

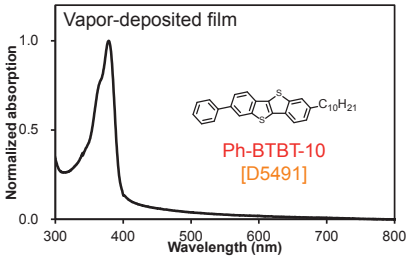

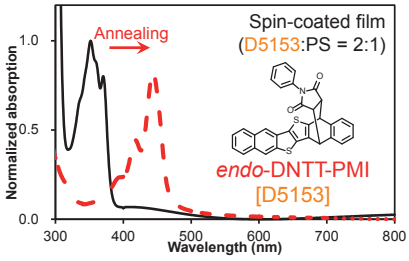

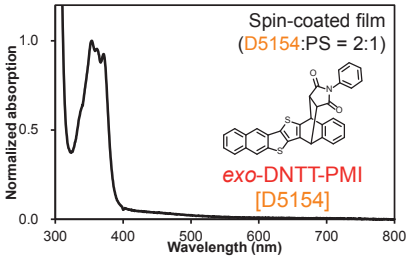

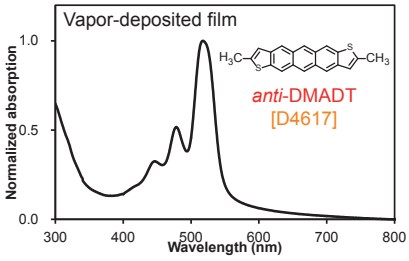

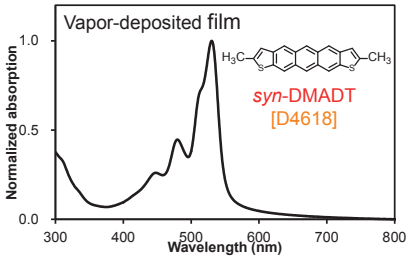

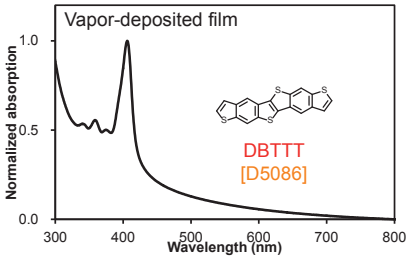

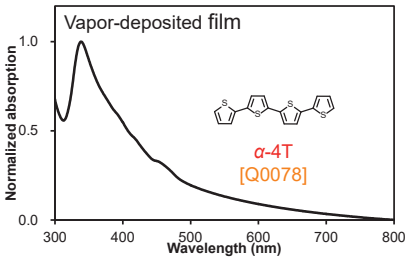

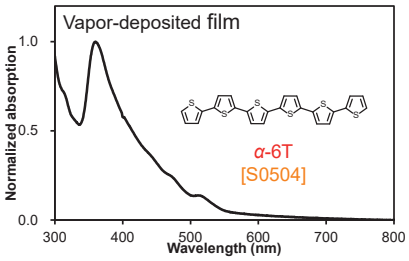

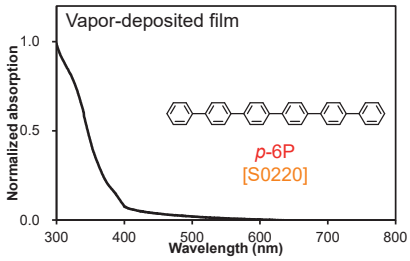

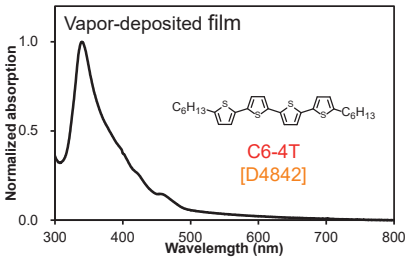

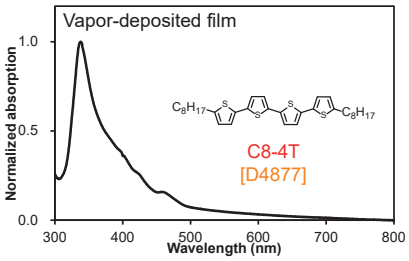

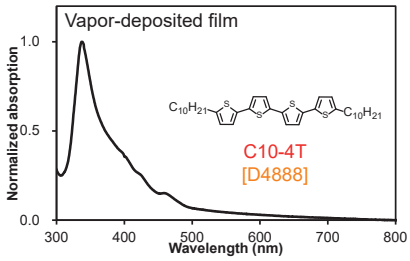

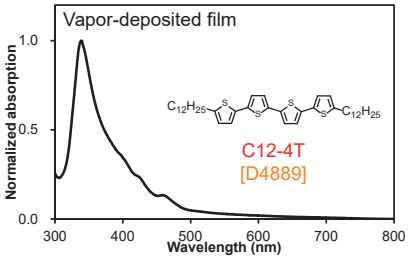

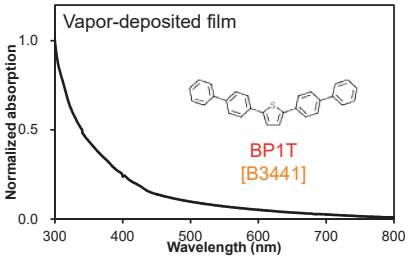

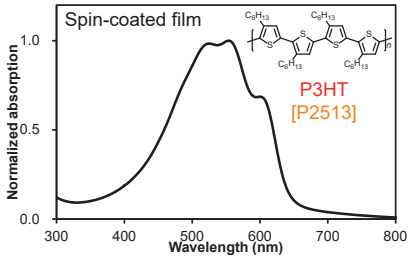

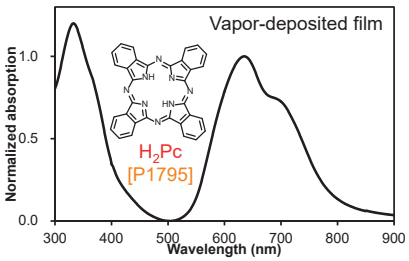

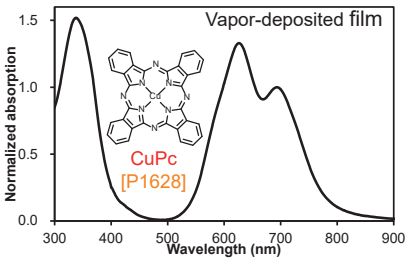

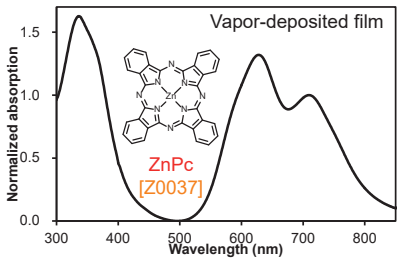

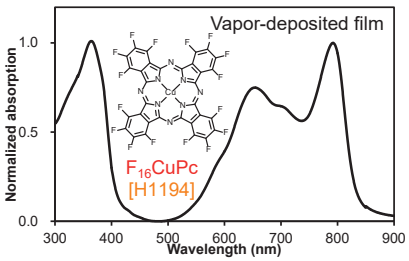

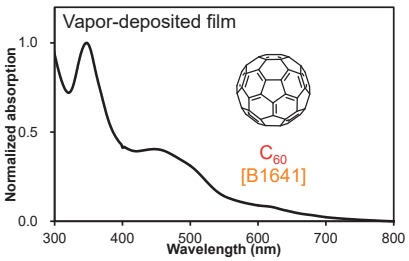

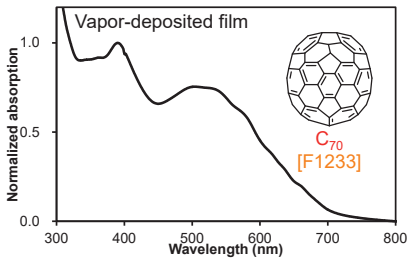

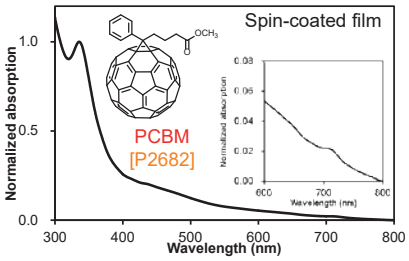

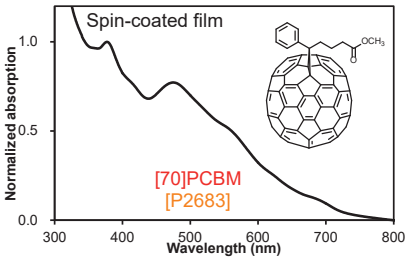

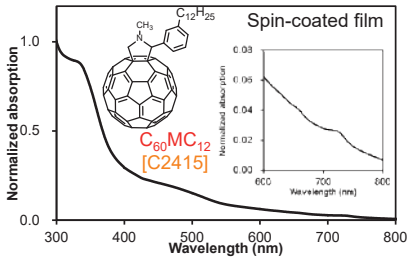

Please inquire for pricing and availability of listed products to our local sales representatives.

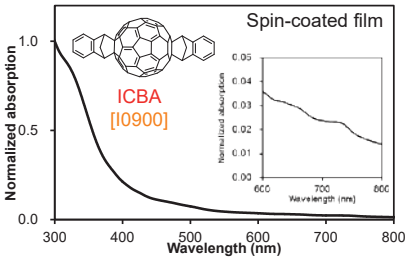
Spin-coated film
ICBA
[I0900]
Normalized absorption
Wavelength (nm)

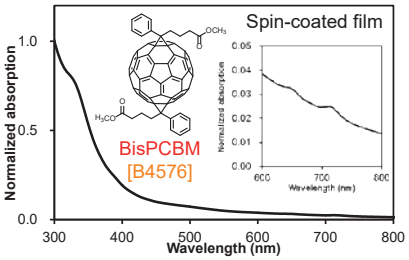
Spin-coated film
BisPCBM
[B4576]
Normalized absorption
Wavelength (nm)

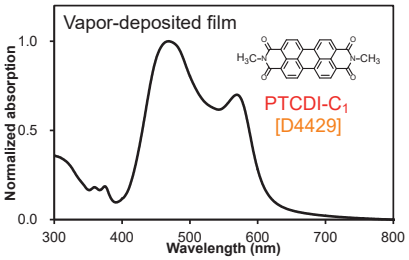
Vapor-deposited film
PTCDI-C1
[D4429]
Normalized absorption
Wavelength (nm)

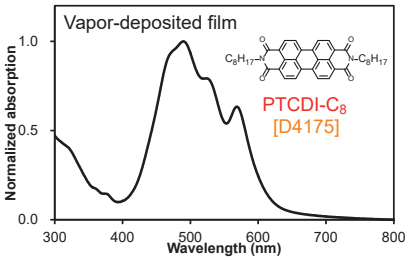
Vapor-deposited film
PTCDI-C8
[D4175]
Normalized absorption
Wavelength (nm)

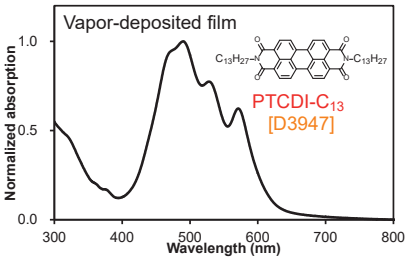
Vapor-deposited film
PTCDI-C13
[D3947]
Normalized absorption
Wavelength (nm)

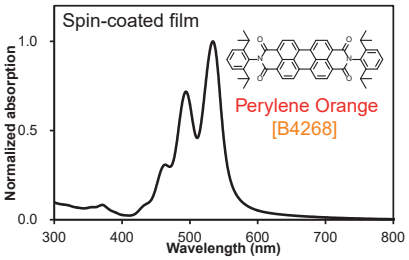
Spin-coated film
Perylene Orange
[B4268]
Normalized absorption
Wavelength (nm)

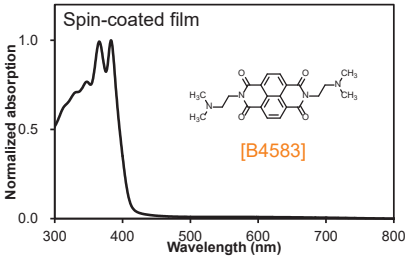
Spin-coated film
[B4583]
Normalized absorption
Wavelength (nm)

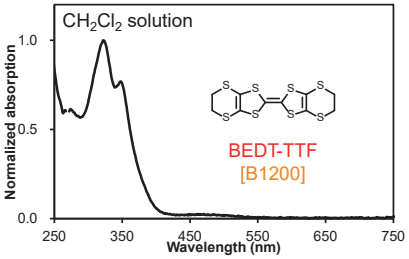
CH2Cl2 solution
BEDT-TTF
[B1200]
Normalized absorption
Wavelength (nm)

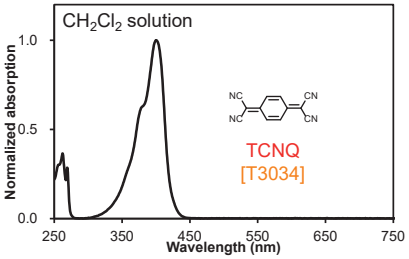
CH2Cl2 solution
TCNQ
[T3034]
Normalized absorption
Wavelength (nm)

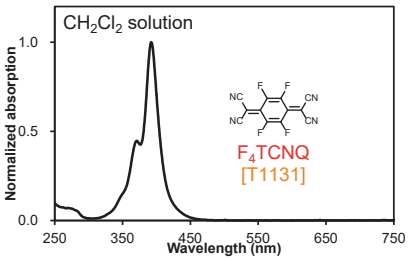
CH2Cl2 solution
F4TCNQ
[T1131]
Normalized absorption
Wavelength (nm)

Energy levels of HOMO

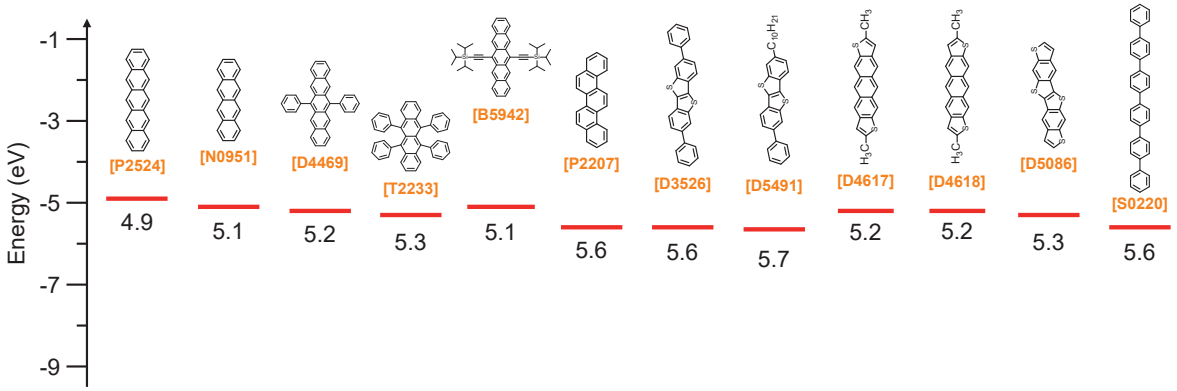

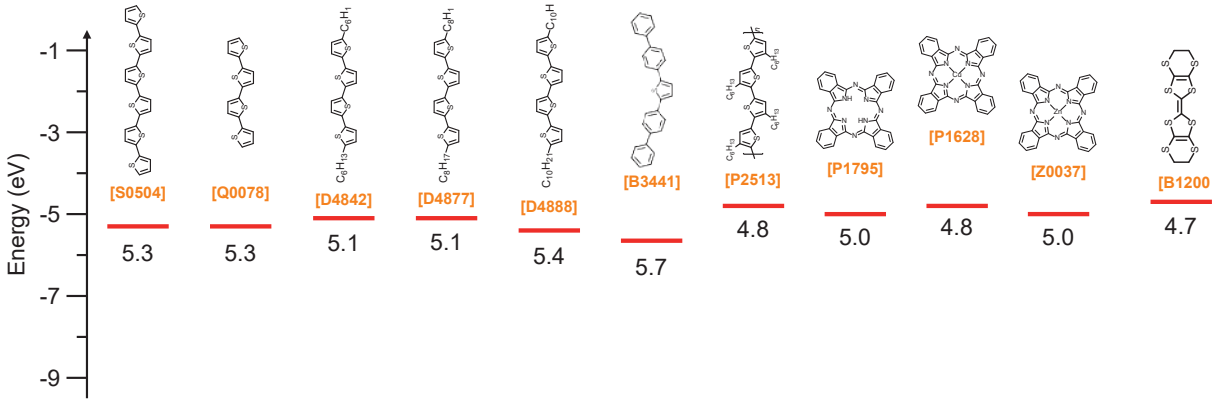

Energy levels of LUMO

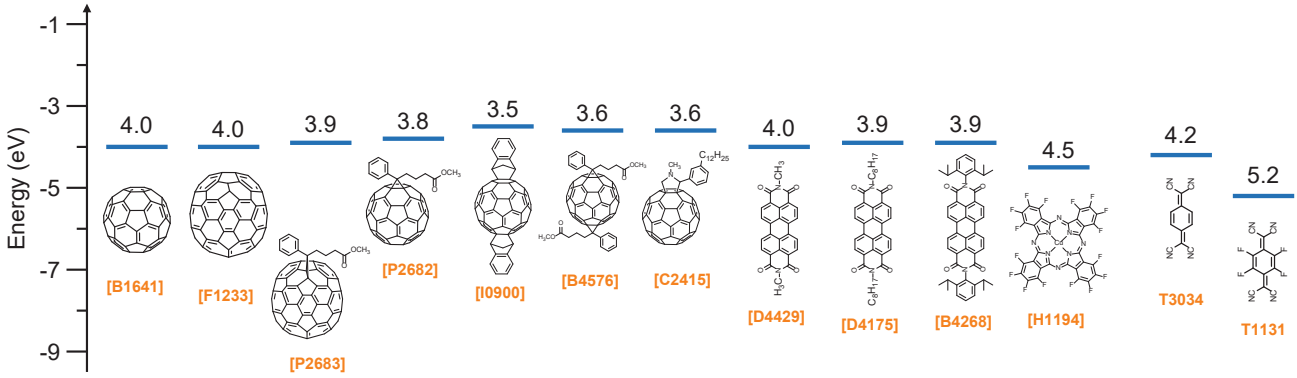

Please inquire for pricing and availability of listed products to our local sales representatives.

Product No.	Compound	LUMO (eV)	HOMO (eV)	*Eg* (eV)	Reference
N0951	Tetracene		5.1		20)
P2524	Pentacene		4.9		20)
T2233	Rubrene		5.3		20)
D4469	6,13-Diphenylpentacene	3.2	5.2	2.0	21)
B5942	TIPS-Pentacene	3.4	5.1	1.8	22)
P2207	Picene		5.6		23)
D3526	DPh-BTBT	2.4	5.6	3.2	24)
D5491	Ph-BTBT-10		5.7		25)
D4617	*anti*-DMADT	3.1	5.2		26)
D4618	*syn*-DMADT	3.0	5.2		26)
D5086	DBTTT	2.4	5.3	2.9	27)
S0220	6P	1.8	5.6	3.8	28)
S0504	6T	3.1	5.3	2.2	29)
Q0078	4T		5.3		30)
D4842	C6-4T		5.1	2.7	31)
D4877	C8-4T		5.1	2.7	31)
D4888	C10-4T	2.6	5.4		32)
B3441	BP1T		5.7		33)
P2513	P3HT		4.8		34)
P1628	CuPc	2.7	4.8	2.2	35)
P1795	H_2PC	2.7	5.0	2.2	35)
Z0037	ZnPc		5.0		36)
B1200	BEDT-TTF		4.7		37)
B4576	Bis-PCBM	3.6	6.0	2.4	38)
I0900	ICBA	3.5	6.0	2.5	38)
B1641	C_{60}	4.0	6.4	2.4	38)
F1233	C_{70}	4.0	6.4		38)
P2682	[60]PCBM	3.8	6.2		38)
P2683	[70]PCBM	3.8	5.9		38)
C2415	$C_{60}MC_{12}$	3.6			39)
D4429	PTCDI-C1	4.0	6.6	2.6	40)
H1194	$F_{16}CuPc$	4.5	6.3	1.8	40)
D4175	PTCDI-C_8	3.9	6.3	2.4	41)
B4268	Perylene Orange	3.9	6.2	2.3	42)
T3034	TCNQ	4.2			43)
T1131	F_4-TCNQ	5.2			44)

References

1) K. Kudo, M. Yamashinaand, T. Moriizumi, *Jpn. J. Appl. Phys*. **1984**, *23*, 130.
2) Y. Y. Lin, D. J. Gundlach, S. F. Nelson and T. N. Jackson, *IEEE Trans. Electron Devices* **1997**, *44*, 1325.
3) M. Kaltenbrunner, T. Sekitani, J. Reeder, T. Yokota, K. Kuribara, T. Tokuhara, M. Drack, R. Schwödiauer, I. Graz, S. Bauer-Gogonea, S. Bauer, T. Someya, *Nature* **2013**, *499*, 458.
4) B. Chu, W. Burnett, JW. Chung, Z. Bao, *Nature* **2017**, *355*, 328.
5) A. C. Arias, J. D. MacKenzie, I. McCulloch, J. Rivnay, A. Salleo, *Chem. Rev*. **2010**, *110*, 3.
6) B. Kang, W. H. Lee, K. Cho, *ACS Appl. Mater. Interfaces* **2013**, *5*, 2302.
7) K. Fukuda, T. Someya, *Adv. Mater*. **2017**, *29*, 1602736.
8) J. G. Mei, Y. Diao, A. L. Appleton, L. Fang, Z. N. Bao, *J. Am. Chem. Soc.* **2013**, *135*, 6724.
9) K. Takimiya, H. Ebata, K. Sakamoto, T. Izawa, T. Otsubo, Y. Kunugi, *J. Am. Chem. Soc*. **2006**, *128*, 12604.
10) H. Iino, T. Usui, J.-I. Hanna, *Nat. Commun*. **2015**, *6*, 6828.
11) R. Ruiz, D. Choudhary, B. Nickel, T. Toccoli, K.-C. Chang, A. C. Mayer, P. Clancy, J. M. Blakely, R. L. Headrick, S. Iannotta, G. G. Malliaras, *Chem. Mater*. **2004**, *16*, 4497.
12) B. Nickel, M. Fiebig, S. Schiefer, M. Göllner, M. Huth, C. Erlen, P. Lugli, *Phys. Stat. Sol. A* **2008**, *205*, 526
13) M. Kitamura, Y. Arakawa, *J. Phys.: Condens. Matter*. **2008**, *20*, 184011
14) Q. Wang, R. Takita, Y. Kikuzaki, F. Ozawa, *J. Am. Chem. Soc*. **2010**, *132*, 11420.
15) J.-R. Pouliot, M. Wakioka, F. Ozawa, Y. Li, M. Leclerc, *Macromol. Chem. Phys*. **2016**, *217*, 1493.
16) R. Zhang, B. Li, M. C. Iovu, M. Jeffries-EL, G. Sauvé, J. Cooper, S. Jia, S. Tristram-Nagle, D. M. Smilgies, D. N. Lambeth, R. D. McCullough, T. Kowalewski, *J. Am. Chem. Soc*. **2006**, *128*, 3480.
17) H. Sirringhaus, P. J. Brown, R. H. Friend, M. M. Nielsen, K. Bechgaard, B. M. W. Langeveld-Voss, A. J. H. Spiering, R. A. J. Janssen, E. W. Meijer, P. Herwig, D. M. de Leeuw, *Nature* **1999**, *401*, 685.
18) J.-F. Chang, B. Sun, D. W. Breiby, M. M. Nielsen, T. I. Sölling, M. Giles, I. McCulloch, H. Sirringhaus, *Chem. Mater*. **2004**, *16*, 4772.
19) L. A. Majewski, J. W. Kingsley, C. Balocco, A. M. Songa, *Appl. Phys. Lett*. **2006**, *88*, 222108.
20) N. Sato, K. Seki, H Inokuchi, *J. Chem. Soc., Faraday Trans. 2* **1981**, *77*, 1621.
21) L. C. Picciolo, H. Murata, Z. H. Kafafi, *Appl. Phys. Lett*. **2001**, *78*, 2378.
22) I. Kaur, W. Jia, R. P. Kopreski, S. Selvarasah, M. R. Dokmeci, C. Pramanik, N. E. McGruer, G. P. Miller, *J. Am. Chem. Soc*. **2008**, *130*, 16274.
23) T. Hosokai, A. Hinderhofer, F. Bussolotti, K. Yonezawa, C. Lorch, A. Vorobiev, Y. Hasegawa, Y. Yamada, Y. Kubozoro, A. Gerlach, S. Kera, F. Schreiber, N. Ueno, *J. Phys. Chem. C* **2015**, *119*, 2902.
24) K. Takimiya, H. Ebata, K. Sakamoto, T. Izawa, T. Otsubo, Y. Kunugi, *J. Am. Chem. Soc*. **2006**, *128*, 12604.
25) M. Kunii, H. Iino, J. Hanna, *Appl. Phys. Lett*. **2017**, *110*, 243301.
26) M. Mamada, T. Minamiki, H. Katagiri, S. Tokito, *Org. Lett.* **2012**, *14*, 4062.
27) J.- II Park, J. W. Chung, J.-Y. Kim, J. Lee, J. Y. Jung, B. Koo, B.-L. Lee, S. W. Lee, Y. W. Jin, S. Y. Lee, *J. Am. Chem. Soc*. **2015**, *137*, 12175.
28) C. Qian, J. Sun, L. Kong, Y. Fu, Y. Chen, J. Wang, S. Wang, H. Xie, H. Huang, J. Yang, Y. Gao, *ACS Photonics* **2017**, *4*, 2573.
29) J. Sakai, T. Taima, T. Yamanari, K. Saito, *Sol. Energy Mater. Sol. Cells* **2009**, *93*, 1149.
30) H. Méndez, G. Heimel, S. Winkler, J. Frisch, A. Opitz1, K. Sauer, B. Wegner, M. Oehzelt, C. Röthel, S. Duhm, D. Többens, N. Koch, I. Salzmann, *Nat. Comm*. **2015**, *6*, 8560
31) M. Ashizawa, T. Niimura, Y. Yu, K. Tsuboi, H. Matsumoto, R. Yamada, S. Kawauchi, A. Tanioka, T. Mori, *Tetrahedron* **2012**, *68*, 2790.
32) S. A. Ponomarenko, S. Kirchmeyer, A Elschner, N. M. Alpatova, M. Halik, H. Klauk, U. Zschieschang, G. Schmid, *Chem. Mater*. **2006**, *18*, 579.
33) T. J. Dingemans, A. Bacher, M. Thelakkat, L. G. Pedersen, E. T. Samulski, H.-W. Schmidt, *Synthetic Metals* **1999**, *105*, 171.
34) V. Vohra, G. Arrighetti, L. Barba, K. Higashimine, W. Porzio, H. Murata, *J. Phys. Chem. Lett*. **2012**, *3*, 1820.
35) D. R. T. Zahn, M. Gorgoi, O. D. Gordan, *Sol. Ener*. **2006**, *80*, 707.
36) W. Tress, K. Leo, M. Riede, *Adv. Funct. Mater*. **2011**, *21*, 2140.
37) N. Sato, G. Saito, H. Inokuchi, *Chem. Phys*. **1983**, *76*, 79.
38) H. Yoshida, *J. Phys. Chem. C* **2014**, *118,* 24377.
39) M. Chikamatsu, A. Itakura, Y. Yoshida, R. Azumi, K. Yase, *Chem. Mater*. **2008**, *20*, 7365.
40) D. R. T. Zahn, G. N. Gavrila. M. Gorgoi, *Chem. Phys*. **2006**, *325*, 99.
41) B. A. Jones, A. Facchetti, M. R. Wasielewski, T. J. Marks, *J. Am. Chem. Soc*. **2007**, *129*, 15259.
42) I. Kim, H. M. Haverinen, Z. Wang, S. Madakuni, J. Li, G. E. Jabbour, *Appl. Phys. Lett*. **2009**, **95**, 023305.
43) K. Kanai, K, Akaike, K. Koyasu, K. Sakai, T. Nishi, Y. Kamizuru, T. Nishi, Y. Ouchi, K. Seki, *Appl. Phys. A* **2009**, **95**, 309.
44) W. Gao, A. Kahn, *Appl. Phys. Lett*. **2001**, *79*, 4040.

High Quality Organic Semiconductor Materials

P2524 100mg 1g

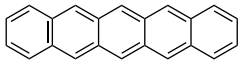

Pentacene (99.999%, trace metals basis) (purified by sublimation)
CAS RN: 135-48-8

D5491 100mg 250mg

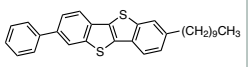

Ph-BTBT-10
CAS RN: 1398395-83-9

P2513 100mg 500mg

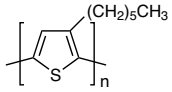

P3HT (regioregular)
CAS RN: 125321-66-6

P2682 100mg

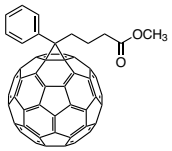

PCBM [for organic electronics]
CAS RN: 160848-22-6

F1233 100mg

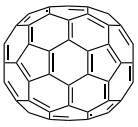

Fullerene C_{70}
[for organic electronics]
CAS RN: 115383-22-7

P2683 100mg

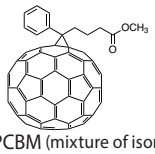

[70]PCBM (mixture of isomers)
[for organic electronics]
CAS RN: 609771-63-3

p-Type Organic Semiconductors

N0001 100mg 1g 5g

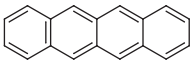

Naphthacene
CAS RN: 92-24-0

N0951 200mg 1g

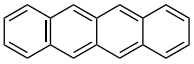

Naphthacene
(purified by sublimation)
CAS RN: 92-24-0

P0030 100mg 1g

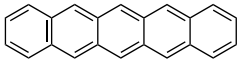

Pentacene (purified by sublimation)
CAS RN: 135-48-8

P2524 100mg 1g

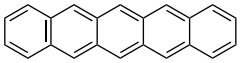

Pentacene (99.999%, trace metals basis) (purified by sublimation)
CAS RN: 135-48-8

D5152 100mg

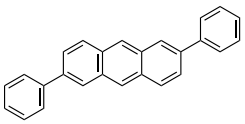

2,6-Diphenylanthracene
(purified by sublimation)
CAS RN: 95950-70-2

T0561 100mg 1g

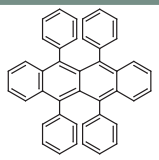

Rubrene
CAS RN: 517-51-1

T2233 250mg 1g

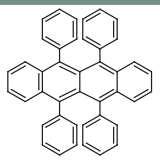

Rubrene (purified by sublimation)
CAS RN: 517-51-1

D4469 200mg

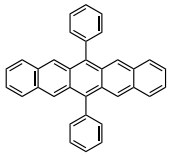

6,13-Diphenylpentacene
CAS RN: 76727-11-2

P2207 100mg

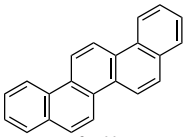

Picene (purified by sublimation) (>99.9%)
CAS RN: 213-46-7

P2383 100mg

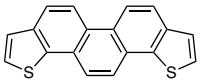

Phenanthro[1,2-*b*:8,7-*b*']-dithiophene
CAS RN: 1491133-64-2

B5551 200mg 1g

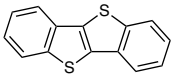

BTBT
CAS RN: 248-70-4

D3526 100mg

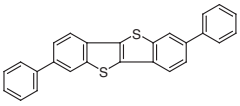

DPh-BTBT (purified by sublimation)
CAS RN: 900806-58-8

D5491 100mg 250mg

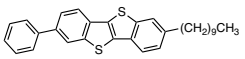

Ph-BTBT-10
CAS RN: 1398395-83-9

D4617 100mg

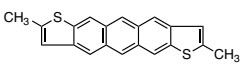

anti-DMADT
(purified by sublimation)
CAS RN: 1019983-99-3

D4618 100mg

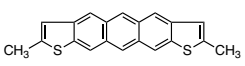

syn-DMADT
(purified by sublimation)
CAS RN: 1392416-39-5

D5153 50mg

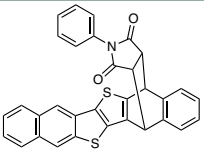

endo-DNTT-PMI (DNTT-Precursor)
CAS RN: 1269669-42-2

D5154 50mg

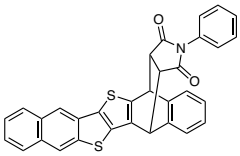

exo-DNTT-PMI (DNTT-Precursor)
CAS RN: 1269669-43-3

B3441 1g 5g

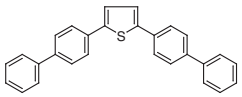

BP_1T
CAS RN: 56316-86-0

H1448 50mg

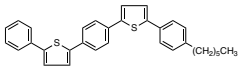

AC5-Hx (purified by sublimation)
CAS RN: 1172135-81-7

D4487 200mg 1g

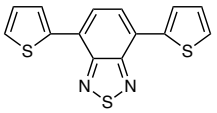

4,7-Di(2-thienyl)-2,1,3-benzothiadiazole
CAS RN: 165190-76-1

B4683 200mg

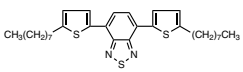

4,7-Bis(5-*n*-octyl-2-thienyl)-2,1,3-benzothiadiazole
CAS RN: 1171974-28-9

S0220 100mg 1g

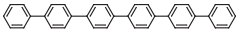

p-Sexiphenyl
CAS RN: 4499-83-6

T1196 1g 5g

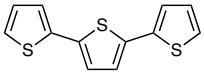

α-Terthienyl
(purified by sublimation)
CAS RN: 1081-34-1

Q0078 100mg

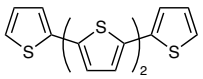

α-Quaterthiophene
CAS RN: 5632-29-1

Q0079 100mg 500mg

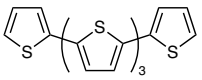

α-Quinquethiophene
CAS RN: 5660-45-7

S0504 100mg 1g

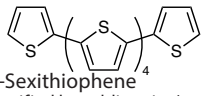

α-Sexithiophene
(purified by sublimation)
CAS RN: 88493-55-4

S0505 100mg

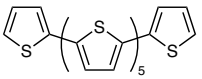

α-Septithiophene
CAS RN: 86100-63-2

O0313 100mg

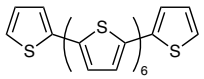

α-Octithiophene
CAS RN: 113728-71-5

P2513 100mg 500mg

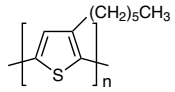

P3HT (regioregular)
CAS RN: 125321-66-6

D4842 100mg

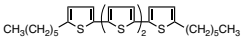

α,ω-Dihexylquaterthiophene
CAS RN: 132814-92-7

D4877 100mg

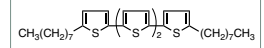

5,5''''-Di-n-octyl-2,2':5',2'':5'',2'''-quaterthiophene
CAS RN: 882659-01-0

D4888 100mg

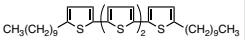

5,5''''-Didecyl-2,2':5',2'':5'',2'''-quaterthiophene
CAS RN: 514188-77-3

D4889 100mg

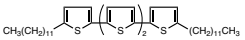

5,5''''-Didodecyl-2,2':5',2'':5'',2'''-quaterthiophene
CAS RN: 153561-79-6

P1795 1g

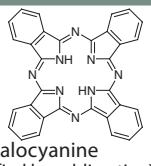

Phthalocyanine
(purified by sublimation)
CAS RN: 574-93-6

P1628 1g

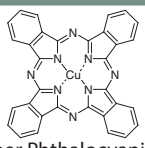

Copper Phthalocyanine
(purified by sublimation)
CAS RN: 147-14-8

P0767 1g 5g 25g

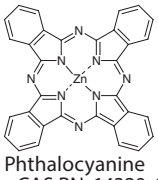

Zinc Phthalocyanine
CAS RN: 14320-04-8

Z0037 500mg

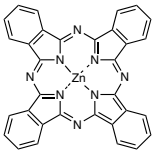

ZnPc (purified by sublimation)
CAS RN: 14320-04-8

B1200 100mg 1g 5g

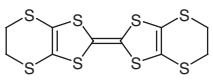

BEDT-TTF
CAS RN: 66946-48-3

n-Type Organic Semiconductors

H1194 100mg 1g

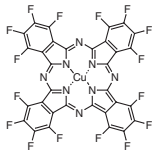

F16CuPc (purified by sublimation)
CAS RN: 14916-87-1

B1641 100mg 1g

Fullerene C_{60} (pure)
CAS RN: 99685-96-8

M2088 100mg

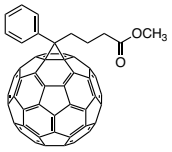

PCBM
CAS RN: 160848-22-6

P2682 100mg

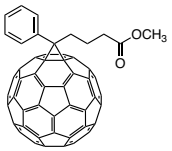

PCBM [for organic electronics]
CAS RN: 160848-22-6

B4576 50mg

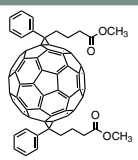

Bis-PCBM (mixture of isomers)
CAS RN: 1048679-01-1

C2415 100mg

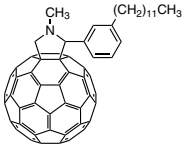

$C_{60}MC_{12}$
CAS RN: 403483-19-2

I0900 50mg

ICBA
CAS RN: 1207461-57-1

B1694 100mg

Fullerene C_{70}
CAS RN: 115383-22-7

F1233 100mg

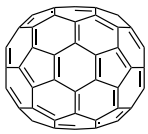

Fullerene C_{70}
[for organic electronics]
CAS RN: 115383-22-7

M2550 50mg

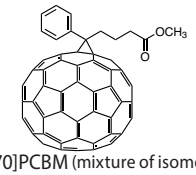

[70]PCBM (mixture of isomers)
CAS RN: 609771-63-3

P2683 100mg

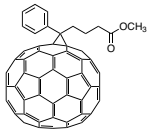

[70]PCBM (mixture of isomers)
[for organic electronics]
CAS RN: 609771-63-3

N0369 25g 250g

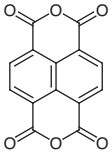

NTCDA
CAS RN: 81-30-1

N0755 1g 5g

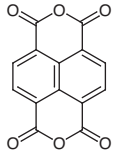

NTCDA (purified by sublimation)
CAS RN: 81-30-1

P0972 25g 100g 500g

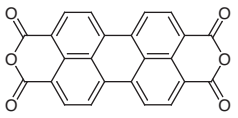

Pigment Red 224
CAS RN: 128-69-8

P2102 1g

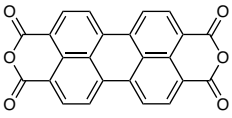

Pigment Red 224
(purified by sublimation)
CAS RN: 128-69-8

D4429 1g 5g

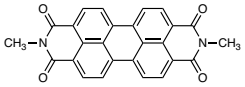

Pigment Red 179
CAS RN: 5521-31-3

D4175 1g

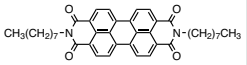

PTCDI-C_8
CAS RN: 78151-58-3

D3947 200mg 1g

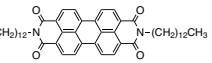

PTCDI-C_{13}
CAS RN: 95689-92-2

B4268 1g 5g

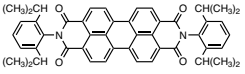

Perylene Orange
CAS RN: 82953-57-9

B4583 200mg

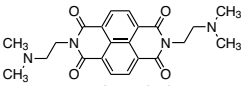

N,N'-Bis[2-(dimethylamino)-ethyl]-1,8:4,5-naphthalene-tetracarboxdiimide
CAS RN: 22291-04-9

T0078 5g 25g

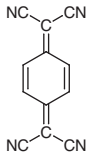

TCNQ
CAS RN: 1518-16-7

T1131 100mg 1g

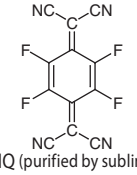

F_4TCNQ (purified by sublimation)
CAS RN: 29261-33-4

Ambipolar Semiconductors

B4361 1g

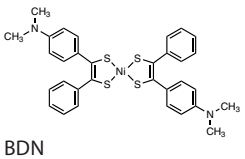

BDN
CAS RN: 38465-55-3

B3612 100mg

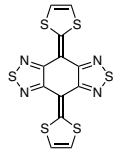

BTQBT (purified by sublimation)
CAS RN: 135704-54-0

C2780 200mg

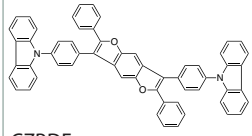

CZBDF
CAS RN: 1092578-51-2

Please inquire for pricing and availability of listed products to our local sales representatives.

T3042 50mg 200mg

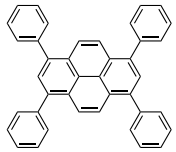

1,3,6,8-Tetraphenylpyrene
CAS RN: 13638-82-9

Liquid Crystalline Semiconductors

D5491 100mg 250mg

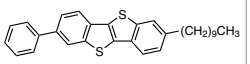

Ph-BTBT-10
CAS RN: 1398395-83-9

D4842 100mg

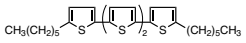

α,ω-Dihexylquaterthiophene
CAS RN: 132814-92-7

D4877 100mg

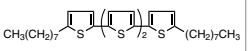

5,5'''-Di-n-octyl-2,2':5',2'':5'',2'''-quaterthiophene
CAS RN: 882659-01-0

D4888 100mg

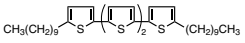

5,5'''-Didecyl-2,2':5',2'':5'',2'''-quaterthiophene
CAS RN: 514188-77-3

D4889 100mg

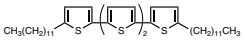

5,5'''-Didodecyl-2,2':5',2'':5'',2'''-quaterthiophene
CAS RN: 153561-79-6

B4683 200mg

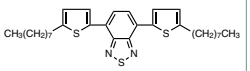

4,7-Bis(5-*n*-octyl-2-thienyl)-2,1,3-benzothiadiazole
CAS RN: 1171974-28-9

H1449 200mg 1g

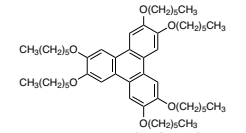

2,3,6,7,10,11-Hexakis(hexyloxy)-triphenylene
CAS RN: 70351-86-9

H1450 200mg 1g

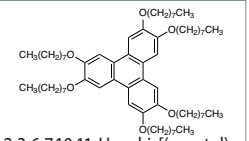

2,3,6,7,10,11-Hexakis[(*n*-octyl)-oxy]triphenylene
CAS RN: 70351-87-0

Ordering and Customer Service

TCI AMERICA
Tel : 800-423-8616 / 503-283-1681
Fax : 888-520-1075 / 503-283-1987
E-mail : Sales-US@TCIchemicals.com

TCI EUROPE N.V.
Tel : +32 (0)3 735 07 00
Fax : +32 (0)3 735 07 01
E-mail : Sales-EU@TCIchemicals.com

TCI Deutschland GmbH
Tel : +49 (0)6196 64053-00
Fax : +49 (0)6196 64053-01
E-mail : Sales-DE@TCIchemicals.com

Tokyo Chemical Industry UK Ltd.
Tel : +44 (0)1865 784560
Fax : +44 (0)1865 784561
E-mail : Sales-UK@TCIchemicals.com

TCI Chemicals (India) Pvt. Ltd.
Tel : 1800 425 7889 / 044-2262 0909
Fax : 044-2262 8902
E-mail : Sales-IN@TCIchemicals.com

梯希爱(上海)化成工业发展有限公司
Tel : 800-988-0390 / 021-67121386
Fax : 021-6712-1385
E-mail : Sales-CN@TCIchemicals.com

TOKYO CHEMICAL INDUSTRY CO., LTD.
Tel : +81 (0)3-5640-8878
Fax : +81 (0)3-5640-8902
E-mail : globalbusiness@TCIchemicals.com